THE EFFECT OF NICKEL COATING OF CARBON FIBRE ON THE INFILTRATION PRESSURE REQUIRED TO PRODUCE FIBRE REINFORCED ALUMINIUM

H. Constantin, A. R. Kennedy*, L. T. Harper, M. S. Johnson, N. A. Warrior

Division of Materials, Mechanics and Structures, Faculty of Engineering, University of Nottingham, Nottingham, UK
**Corresponding author (andrew.kennedy@nottingham.ac.uk)*

Keywords: metal matrix composites, carbon fibre, gas pressure infiltration

Abstract

To quantify and compare the wetting behaviour of aluminium on nickel coated and uncoated carbon fibre, composite materials were fabricated by liquid metal infiltration, using a range of gas pressures. The porosity was quantified by image analysis, and compared with data obtained from mercury intrusion porosimetry of preforms of similar structure. Results show that nickel coating significantly reduces the pressure required to fabricate these composite materials, due to improved wetting. However, the nickel coating reacts with the aluminium matrix to form brittle blocky Al_3Ni intermetallic phases.

1. Introduction

The strength of a composite is highly dependent upon the interfacial bonding between the matrix and reinforcement [1, 2]. In the case of aluminium (Al) metal matrix composites (MMCs) reinforced with carbon fibres (CFs), poor wettability and brittle reaction products, such as Al_4C_3, often cause fibre agglomeration, strength loss and composite cracking [3-6].

Liquid infiltration is a process commonly employed for the fabrication of MMCs [4, 5]. Poor wetting between the matrix and reinforcement (contact angles greatly exceeding 90^o [5]) means that an external pressure must be applied for infiltration to take place [6, 7]. Once a particular threshold pressure has been surpassed, liquid metal will penetrate the large interconnected channels, only infiltrating smaller pores at higher pressures [7]. The complex geometry that preforms can take, make understanding the governing phenomena of infiltration difficult [8, 9] as it involves both physical and chemical elements [8]. Drainage curves are frequently used to attempt to model infiltration behaviour, comparing volume intruded with applied pressure, depending on both capillarity parameters such as wetting angle and surface tension, and physical parameters such as pore size and distribution [7]. Drainage curves are difficult to produce for MMCs due to the high temperatures and pressures required for infiltration [5]. Subsequently, drainage curves produced from mercury intrusion porosimetry (MIP) of the same preforms at room temperature, can be used to better understand infiltration behaviour [7].

Coatings can be employed to either improve the wettability between molten Al and CF, or to act as a barrier to reduce or prevent interfacial reactions. Ni-CF/Al has been investigated

previously, exhibiting improved interfacial bonding [10], increased hardness and elastic modulus [11], and more homogeneous distribution of fibres [12] compared with uncoated CF/Al.

As Ni coating clearly has a positive impact on the fabrication and properties of CF/Al, the aim of this study is to quantify the effect of Ni coating on the wettability of Al on CFs. This will be achieved by producing CF/Al composite materials with uncoated and Ni coated-CFs at varying infiltration pressures and relating this to the microstructure of the resulting composites.

2. Methodology

An Al–12Si alloy (LM6) was obtained from Norton Aluminium. HTS40 12K CF and Ni-CF tow were obtained from Toho Tenax. In order to fabricate a preform from a continuous length of CF tow, the CF was crocheted, using a 7mm crochet hook, into a rectangular shape and rolled into a cylinder of diameter 30mm and height 30mm, occupying a total volume of 21.2cc.

MMCs were fabricated by gas pressure infiltration (GPI) using argon (Ar). Al was placed on top of the preform in an alumina crucible and placed inside a pressure vessel. The preform and Al weighed 9.5g and 35g, respectively. The system was heated to 550^{o}C under vacuum for 1 hour to remove sizing from the preforms, to 750^{o}C and held for 1 hour to allow the Al to melt and to seal the preform, where after Ar gas pressure (ranging from 2.5 to 50 bar) was applied for 30 minutes followed by cooling and solidification under pressure. MMCs were sectioned and mounted in conductive resin and polished to a 1μm diamond finish (without the use of water as this may remove possible interfacial reaction products) and were studied using both optical (OM) and scanning electron microscopy (SEM). The volume fraction (VF) of fibres and porosity levels were measured using image analysis (IA) software, Image J. Reaction products and intermetallic phases were quantified using XRD. Drainage curves were produced using a Micrometrics Autopore 4 Hg Porosimeter, performed at pressures ranging from 0.05 to 50 bar, with a 10 second step between each pressure interval.

3. Results and Discussion

Figure 1 shows OM images of end-on fibres from a preform cast in a polymer resin. On a macroscopic level, the preforms are characterised by bundles of densely packed CFs surrounded by void spaces. These large void spaces range considerably in size (see Figure 1 ‘a’ and ‘b’), as some bundles are in contact and others are several millimetres apart. On a microscopic level, bundles contain 12,000 filaments of CF and Ni-CF. IA indicates that Ni-CF intra-bundle VF is 0.67 (0.5 if the Ni-coating is ignored) and for CFs 0.66. The diameters of Ni-CFs and CFs are measured to be 8.7μm (6.6μm without coating) and 6.8μm, respectively; the diameters specified by the manufacturer are 7.5μm (7μm without coating) and 7μm, respectively. The average spacing between fibres, as is the case for the bundles, varies widely (see Figure 1 ‘c’ and ‘d’); the average spacings of 0.31μm for Ni-CF and 0.40μm for CF, with standard deviations of 0.26 and 0.34 respectively, reflecting this wide range. CF has a density of 1.65g/cc, measured by MIP, and when crocheted the preform has an estimated VF of 0.27. The density of Ni-CF is 1.92g/cc and the estimated preform VF (including Ni-coating) is 0.23.

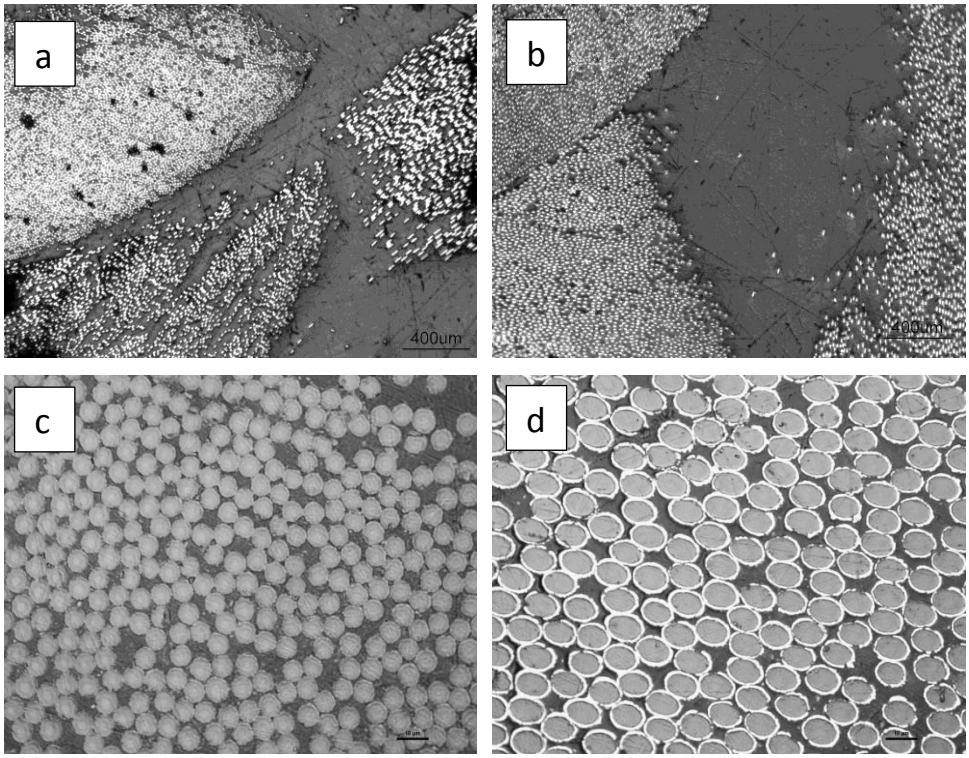

Figure 1. OM images, (a) inter-bundle CF, (b) inter-bundle Ni-CF, (c) intra-bundle CF, (d) intra-bundle Ni-CF

Figure 2 shows a plot of preform saturation versus pressure for MIP and is derived from the ratio of volume intruded at a given pressure, to the maximum intruded volume. The two traces show similar features, albeit with the saturations at any given pressure for Ni-CF preforms translated to higher values. The differences can be attributed to the lower preform VF achieved for the coated fibres, with the VFs and saturations both differing by roughly 15%. Filling begins at 0.06 bar (point 'i' on Figure 2), with a step at 0.23 bar (point 'ii'), briefly plateauing at 1.38 bar (point 'iii'), resuming filling at 2.51 bar and fully saturating at 22.67 bar (point 'iv').

The Young-Laplace equation (Equation 1 [13]) expresses the capillary diameter (d) in terms of the surface tension of the liquid metal (γ_{Hg}), the contact angle between the liquid metal and reinforcement (ϑ) and applied pressure (P). Using values for ϑ for Hg on carbon and γ_{Hg} taken from [13, 14] (124° and 0.485 Nm, respectively), applied pressures of 0.06, 0.23, 1.38, 2.51 and 22.67 equate to capillary diameters of 181, 47, 7.9, 4.3 and 0.48μm, respectively. Of particular interest is point 'iii', which is likely to correspond to a transition between inter- and intra-bundle infiltration. The calculated capillary diameter range at this plateau, of 7.9 – 4.3μm, relating to the pressure marking this transition, is consistent with the largest intra-bundle spacing shown in Figure 1. Complete saturation, point 'iv', equates to a capillary diameter of 0.48μm. This is close to the estimated intra-bundle fibre spacing 0.40μm.

$$d = \frac{4\gamma_{Hg}cos\vartheta}{P} \quad (1)$$

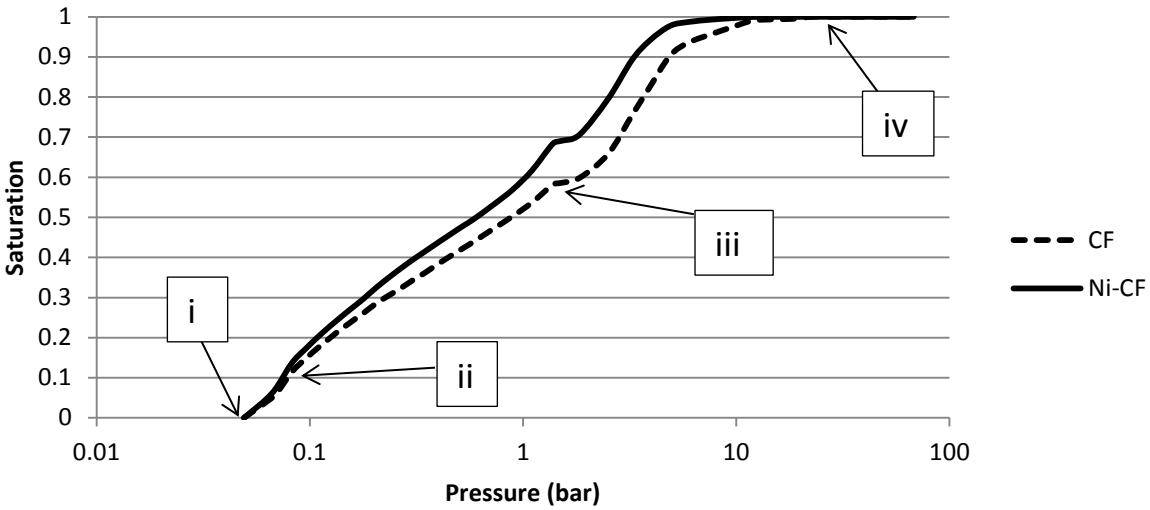

Figure 2. MIP data for crocheted uncoated and Ni-coated CF preforms

In order to translate these plots to an Al system, the applied pressure can be multiplied by a scalar (φ) calculated using equation 2 [6], which relates the surface energies of Hg and Al (γ_{Hg} and γ_{Al}) and the contact angles of Hg and Al on the reinforcement phase ($\vartheta_{Hg/r}$ and $\vartheta_{Al/r}$):

$$\varphi = \frac{\gamma_{Al}\cos\left(\vartheta_{Al/r}\right)}{\gamma_{Hg}cos\left(\vartheta_{Hg/r}\right)} \tag{2}$$

For the CF/Al-12Si system, $\vartheta_{Al/C}$ and γ_{Al} have been taken from [14] as 139° and 0.847 Nm, respectively and thus φ is 2.4. The critical point marking the predicted transition from inter- and intra-bundle infiltration in the Al-12Si system is therefore between 3.3 and 6.0 bar, with complete filling occurring above 54.4 bar. Figure 3 shows the estimated porosity obtained from the saturation data from MIP, translated to the (Al) system. Porosities measured by IA of MMCs have also been presented and agreement is poor. The IA method can prove erroneous given the range of different magnifications required to capture representative regions of the composite, due to the difficulties thresholding the fibres separately from polishing artefacts.

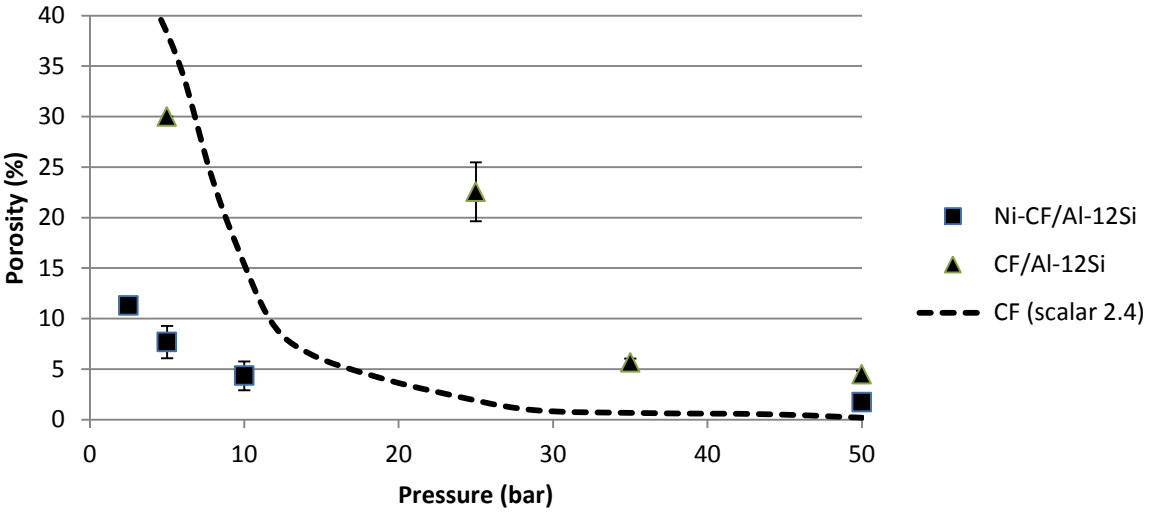

Figure 3. Scaled MIP data with porosity data obtained from microscopy of MMCs

Despite poor correlation between IA measurements of porosity and the predicted infiltration behaviour, microstructural evaluation of the extent of infiltration at different pressures does have a much closer bearing. Figure 4 compares the porosity for CF/Al-12Si MMCs processed at different pressures. At 5 bar, only the inter-bundle spaces have been infiltrated. This pressure is below the predicted intra-bundle threshold pressure of 6.0 bar calculated from MIP and translated to the Al system. At 25 bar, partial intra-bundle infiltration occurs, but large intra-bundle voids are still present. The drop in porosity between MMCs produced at 25 bar and 35 bar is significant and at 50 bar (close to the estimated 54 bar required) intra-bundle infiltration is almost complete. This can be seen clearly in Figure 5, which shows the centre of a fibre bundle filled with Al.

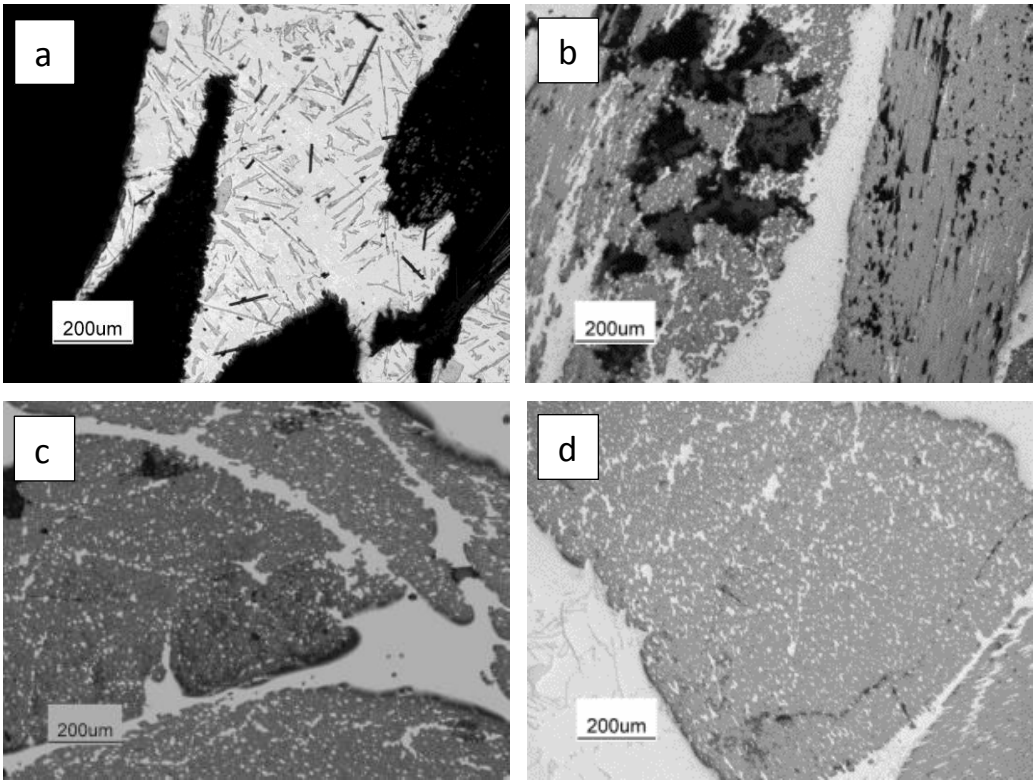

Figure 4. OM images of CF/Al-12Si processed using (a) 5 bar, (b) 25 bar, (c) 35 bar, (d) 50 bar gas pressure

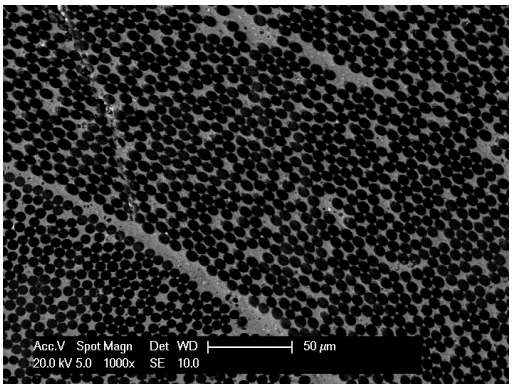

Figure 5. SEM image of CF/Al-12Si processed using 50 bar gas pressure

It is clear from Figure 3 that Ni-coating encourages more complete infiltration at any given pressure and Figure 6 presents the porosity for Ni-CF/Al-12Si MMCs processed at different pressures. At 2.5 bar, the porosity is lower than CF/Al-12Si processed at 25 bar. At 5 bar, the voids are confined to the centres of the bundles. At 10 and 50 bar, fibre bundles appear well infiltrated and almost free of porosity (see Figure 7). This image shows that the Ni coating has been removed from the fibres, and can be seen in white as part of the Al matrix.

The intra-bundle VF of Ni-CFs post-infiltration is 0.49, close in value to the pre-infiltration intra-bundle VF of 0.5 (excluding Ni-coating). Conversely, the VF of uncoated CFs pre- and post- infiltration increases from 0.66 to 0.77. This suggests that the uncoated CFs have agglomerated during infiltration; most likely due to poor wetting, in agreement with Rams et al [11].

As the geometries and packing fractions within the fibre bundles (pre-infiltration) are similar, the significant reductions in infiltration pressure required are attributed to the improved wetting behaviour between the Al matrix and Ni-coated fibres. Although the contact angle for Al on Ni is clearly lower than that for Al on CF, it is not as low as has been measured using the sessile drop method [15, 16] on ceramic materials such as silicon carbide and graphite (31^o and 12^o) respectively, which, by this analysis would lead to infiltration without the use of external pressure. The process used here is clearly very different to the sessile drop measurement technique, with shorter incubation times available for reactive wetting to occur. Additional complications also arise owing to changes in melt properties, composition and preform architecture as the Ni coating dissolves from the fibres.

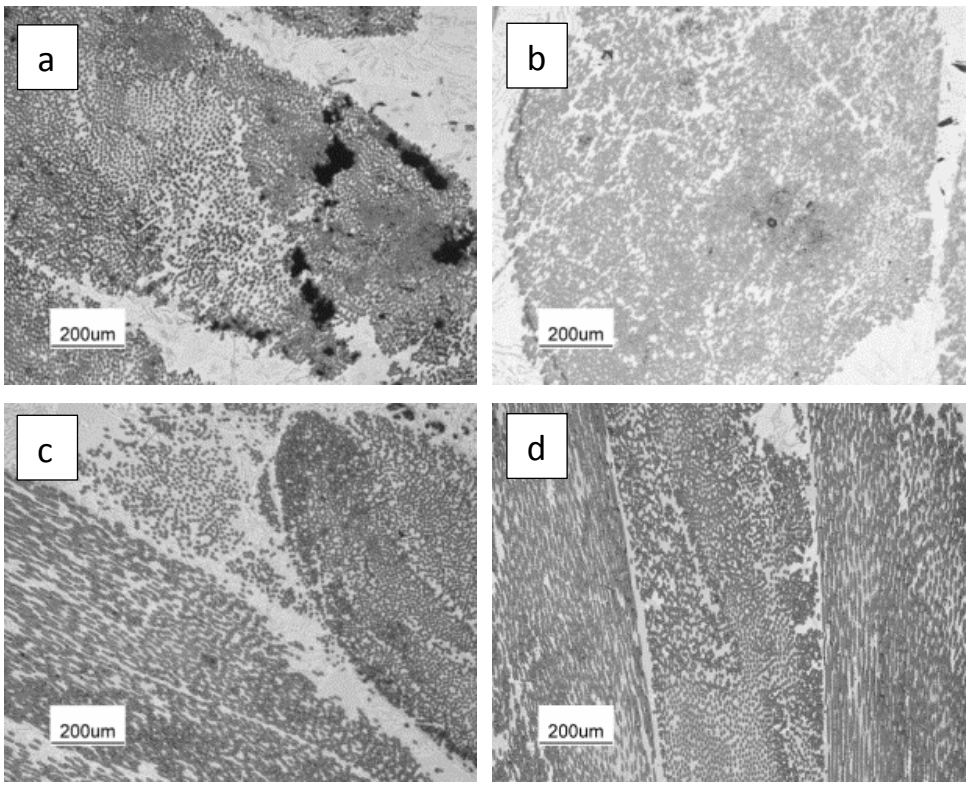

Figure 6. OM images of CF/Al-12Si processed using (a) 2.5 bar, (b) 5 bar, (c) 10 bar, (d) 50 bar gas pressure

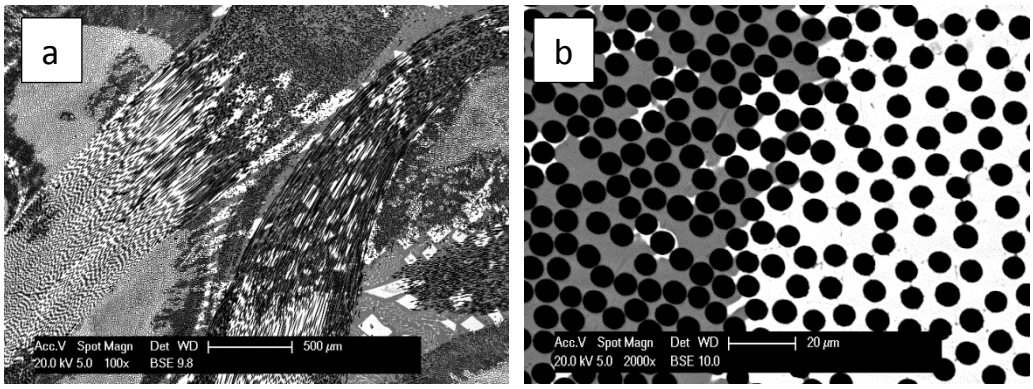

Figure 7. SEM images of Ni-CF/Al-12Si processed using 50 bar gas pressure

The XRD traces in Figure 8 show numerous Al_3Ni peaks present in the MMCs containing Ni-CF. The plots also show some Al_4C_3 peaks present in uncoated-CF MMCs which are absent in Ni-CF MMCs, suggesting that the Ni coating has reduced the formation of Al_4C_3, although such reaction products will most likely have been replaced with brittle Al_3Ni intermetallics. Thus, during infiltration at 750°C, Al and Ni react to form Al_3Ni, dissolution and diffusion of Ni results in the Ni-coating being removed from the fibres (see Figure 7), forming blocky intermetallics within the CF bundles and the matrix-rich regions. These blocky Al_3Ni intermetallics indicate that a hyper-eutectic (>5.7wt%Ni) alloy has formed. From the VF of Ni-CFs and the measured coating thickness, the Ni content in the Al alloy has been estimated at 15.9wt%. These intermetallics are brittle and propagate cracks in the matrix.

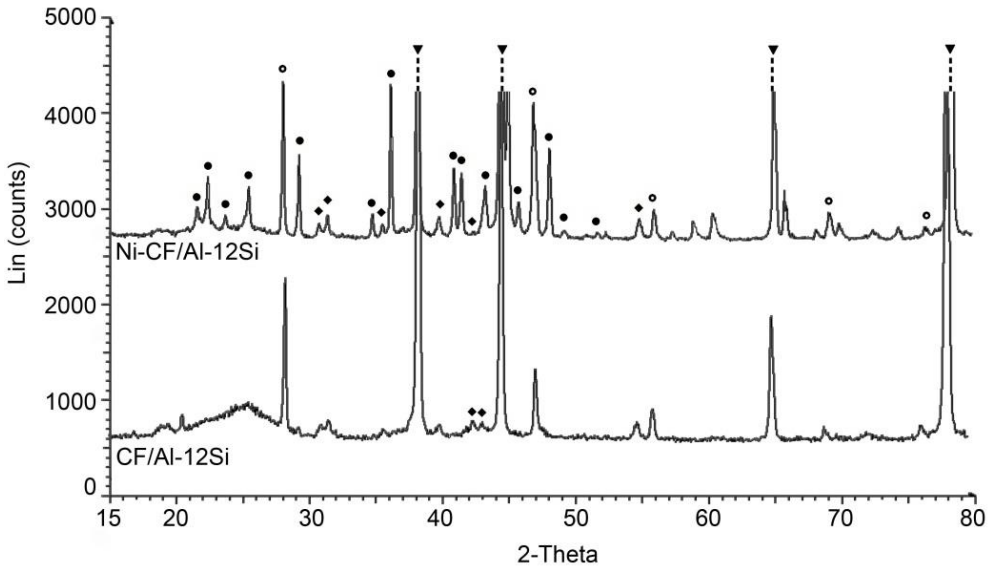

Figure 8. XRD plots of MMCs, ▼ = Al, ○ = Si, • = Al_3Ni, ◆ = Al_4C_3

5. Conclusions

Several conclusions can be drawn from this piece of work:

1. MMCs can be fabricated using crocheted preforms at infiltration pressures below 50 bar
2. MIP can be used to predict the saturation behaviour of these preforms, which consists of 2 distinct phases – inter-bundle and intra-bundle infiltration

3. Ni coating on CF reduces the pressure required to fabricate MMCs by approximately 5 times; this is due to the improved wetting behaviour between molten Al and Ni, and has the added benefit of reducing intra-bundle densification
4. The Ni coating reduces the formation of Al_4C_3, however the coating does not remain on the fibres during the fabrication process; it reacts with the Al matrix to form blocky Al_3Ni intermetallics. The Ni content must be reduced to minimise formation of this phase.

The authors gratefully acknowledge financial support of this research from the Engineering and Physical Sciences Research Council, project TARF-LCV, EP/1038616/1

6. References

1. Schwarz, B., C. Eisenmenger-Sittner, and H. Steiner, Construction of a high-temperature sessile drop device. Vacuum, 82: p. 186 - 188.2008
2. Mortensen, A., Interfacial phenomena in the solidification processing of metal matrix composites. Materials Science and Engineering: A, 135: p. 1 - 11.1991
3. Wang, J., et al., A combined process of coating and hybridizing for the fabrication of carbon fiber reinforced aluminum matrix composites. Composites Part A: Applied Science and Manufacturing, 28(11): p. 943-948.1997
4. Michaud, V. and A. Mortensen, On measuring wettability in infiltration processing. Scripta Materialia, 56(10): p. 859-862.2007
5. Bahraini, M., et al., Measuring and tailoring capillary forces during liquid metal infiltration. Current Opinion in Solid State and Materials Science, 9(4–5): p. 196-201.2005
6. Bahraini, M., et al., Wetting in infiltration of alumina particle preforms with molten copper. Journal of Materials Science, 40: p. 2487 - 2491.2005
7. Despois, J.F., et al., Influence of the infiltration pressure on the structure and properties of replicated aluminium foams. Materials Science and Engineering: A, 462(1–2): p. 68-75.2007
8. Dopler, T., A. Modaressi, and V. Michaud, Simulation of metal-matrix composite isothermal infiltration processing. Metallurgical and Materials Transactions B, 31B: p. 225 - 234.2000
9. Kaufman, H. and A. Mortensen, Wetting of SAFFIL alumina fibre preforms by aluminium at 973K. Metallurgical Transactions A, 23: p. 2071 - 2073.1992
10. Ren, F.-z., et al., Effect of interface properties on the mechanical performance of carbon fiber/Mg composites fabricated by powder metallurgy. Carbon, 50(1): p. 343.2012
11. Rams, J., et al., Electroless nickel coated short carbon fibres in aluminium matrix composites. Composites Part A: Applied Science and Manufacturing, 38(2): p. 566-575.2007
12. Ramesh, C.S., et al., Tribological characteristics of innovative Al6061–carbon fiber rod metal matrix composites. Materials & Design, 50(0): p. 597-605.2013
13. Gil, R., A. Jinnapat, and A.R. Kennedy, Pressure-assisted infiltration of molten aluminium into open cell ceramic foams: Experimental observations and infiltration modelling. Composites Part A: Applied Science and Manufacturing, 43: p. 880 - 884.2012
14. Molina, J.M., et al., Infiltration of graphite preforms with Al–Si eutectic alloy and mercury. Scripta Materialia, 56(11): p. 991-994.2007
15. León, C.A. and R.A.L. Drew, The influence of nickel coating on the wettability of aluminum on ceramics. Composites Part A: Applied Science and Manufacturing, 33(10): p. 1429-1432.2002
16. Ip, S.W., et al., Wettability of nickel coated graphite by aluminum. Materials Science and Engineering: A, 244(1): p. 31-38.1998